

A Novel Installation Parameter Optimization Design Method of Forming Tool for Screw Rotor

Zongmin Liu (✉ liu_zm@ctbu.edu.cn)

Chongqing Technology and Business University

Jirui Wang

Qian Tang

Ning Liu

<https://orcid.org/0000-0002-8517-0652>

Bin Xing

Research Article

Keywords: screw rotor, forming tool, cutting performance, design method

Posted Date: February 7th, 2022

DOI: <https://doi.org/10.21203/rs.3.rs-1308630/v1>

License:   This work is licensed under a Creative Commons Attribution 4.0 International License.

[Read Full License](#)

A Novel Installation Parameter Optimization Design Method of

Forming Tool for Screw Rotor

Zongmin Liu ^{1,2,5}, Jirui Wang ², Qian Tang ³, Ning Liu ^{4,*}, Bin Xing ^{5*}

¹ National Research Base of Intelligent Manufacturing, Chongqing Technology and Business University, Chongqing 40006.

² School of Mechanical Engineering, Chongqing Technology and Business University, Chongqing 400067.

³ School of Mechanical and Vehicle Engineering, Chongqing University, Chongqing 400067.

⁴ Virtual Manufacturing Group, Smart Manufacturing Division, Advanced Remanufacturing and Technology Centre, 3 Cleantech Loop, #01-01, CleanTech Two, Singapore 637143.

⁵ Chongqing Industrial Big Data Innovation Center Co. LTD, Chongqing 400067.

* Correspondence: Liu_Ning@artc.a-star.edu.sg; Tel.: +65-96517567

Correspondence: Xing.bin@hotmail.com; Tel.: +86-18601118819

Abstract

Characterized by a complex contour profile involving arc, cycloid and involute, etc., the screw rotor is usually manufactured by a forming tool. The finished surface quality and efficiency of the screw rotor are determined by the cutting performance of the forming tool. However, the machining performance of the forming tool is closely related to the structure shape of cutting edge, which is then determined by the installation parameters of the forming tool. Therefore, to make the cutting performance of forming tool controllable, it is essential investigate the relationship between the cutting performance of the forming tool and its installation parameters at the design stage. In this paper, a novel installation parameter optimization design method of forming tool for screw rotor is presented. A parametric optimization program is designed to finalize the range of installation parameters satisfying the spatial meshing relation and machining equipment parameters. The profile characteristics of forming tool under different center distances and mounting angles have been investigated. For validation, several screw rotors were ground in experiments and the resulted profile errors were analyzed. The results show that the cost of precision grinding of screw rotor can be significantly reduced, without compromise of machining quality. As such, the proposed design method could serve as a promising platform to facilitate screw rotor manufacture.

Keywords: screw rotor; forming tool; cutting performance; design method

1. Introduction

The screw rotor is the core component of screw machinery (e.g., screw pump/compressor/vacuum pump/expander), and its manufacturing accuracy has a direct influence on the comprehensive performance of screw machinery [1]. Undesired profile errors will lead to a wide series of degraded performance including poor sealing, excessive noise and vibration, and reduced wear resistance. Therefore, in real production, the tooth profile accuracy of the screw rotor is required to be extremely high. As such, forming processing has become the most commonly used processing method in screw rotor manufacture, due to its controllable processing accuracy and convenience in rotor profile modification. The mounting parameters of the forming tool can directly determine the attitude of the spatial contact line between the forming tool and the screw rotor, thus further affect the cutting performance of the forming tool. Therefore, to obtain reasonable mounting parameters

41 becomes the prerequisite in the design of forming tool. Unfortunately, in traditional screw rotor
42 forming tool design, the mounting parameters are usually obtained by empirical methods. Such
43 methods often lead to poor cutting performance of the forming tool, which will further affect the
44 machining accuracy and efficiency in screw rotor manufacture. In order to achieve robust
45 manufacture of screw rotor, it is essential to optimize the cutting performance of the forming tool
46 by selecting appropriate mounting parameters.

47 The design principle and method of forming tools for screw rotors have been described in detail
48 in previous literatures [2,3]. These studies have provided the solution method and the solution step
49 of the screw rotor forming tool profile, and valuable references for the design of screw rotor forming
50 tools are provided. However, unfortunately, there is still a lack in the screw rotor forming tool
51 mounting parameter decision method. Tang et al. [4] proposed a new method of screw rotor forming
52 tool design, which avoids the technical difficulty of discontinuous one-medium derivative of screw
53 rotor profile curve. Wu et al. [5], proposed a radial ray method to design the screw rotor forming
54 grinding wheel. This method firstly solved the forming sand profile from the given screw rotor
55 profile, and then figured out the screw rotor profile from the forming wheel profile, thus realizing
56 the screw rotor profile precision forming grinding simulation. Li [6] proposed a novel calculation
57 process based on the end milling cutter spiral groove machining principle to compute the grinding
58 wheel profile with a known groove model and grinding wheel axis setting parameters. Hoang et al.
59 [7] established a general mathematical model for internal-meshing honing for screw rotors.
60 Furthermore, the proposed mathematical model has been verified to honing screw rotors with
61 constant lead and variable lead. Bizzarri and Bartoň [8] proposed a method for machining screw
62 rotors with double-flank milling on the five-axis machine tool, and verified the feasibility of this
63 method on several existing screw rotors. While these studies have provided valuable information
64 and useful reference on forming tool design methods, they have not addressed the influence of
65 forming tool mounting parameters on the screw rotor profile errors.

66 In contrast, the influence of screw rotor forming tool mounting parameters on screw rotor
67 machining profile errors were revealed in another group of studies. Stosic [9-10], for example,
68 proposed a method for calculating the wear amount of a screw rotor forming milling tool, and
69 obtained the influence of the tool wear on the profile error of the screw rotor through the method of
70 transforming the space coordinate system. In this study, considering the tool and the screw rotor
71 have different relative motion speeds at different contact points, the cutting process would result in
72 different tool wear levels. In a subsequent study, Stosic illustrated the influence of installation angle,
73 axial deviation and center distance on the profile error of the screw rotor. Tao et al. [11] proposed a
74 method to evaluate the screw rotor profile error caused by the installation parameter error of forming
75 grinding wheel, including the installation angle error, center distance error and axial displacement
76 error. Both single factor and coupling factors were comprehensively investigated in this method.
77 Zhao et al. [12], who investigated the influence of multiple factors on screw rotor profile error in
78 CNC precision forming grinding of screw rotor, further proposed a new CNC grinding wheel
79 segmentation dressing method to improve screw rotor grinding precision and efficiency. Hoang and
80 Wu [13] established a general coordinate system for simulating the machining of single-thread screw
81 rotor with end milling cutter on a multi-axis CNC milling machine. The machining accuracy of the
82 rotor can be improved by using different combinations of end mill tool installation parameters or
83 tool profile corrections. They then performed machining experiments or simulation experiments to
84 verify the correctness of the proposed method.

85 Current research is focusing on the mechanism of the screw rotor profile error, meanwhile, other
86 researchers have also proposed the compensation method of the screw rotor profile error [14-16].
87 Representatively, on the basis of studying the generation of profile error of the screw rotor, Liu et
88 al. [17] proposed a profile error compensation method caused by the wear of the forming wheel.
89 This method was realized by adjusting the installation parameters of the forming wheel, which
90 improved the precision forming grinding efficiency. These researchers have attempted to improve
91 the machining accuracy of the screw rotor by controlling the mounting parameters of the forming
92 tool. On the one hand, the reported models are helpful to improve the profile accuracy of the screw
93 rotor to some extent. On the other hand, these models are established based on a common
94 assumption that the forming tool mounting parameters and profile have been pre-determined.
95 Furthermore, the design method of mounting parameters of the screw rotor forming tool has not
96 been well described in the above studies. In order to overcome the problem of interference between
97 tool and rotor profile during machining of concave rotor profile. Zhang and Fong [18] proposed a
98 novel tilt form grinding (TFG) method. By using their proposed mounting parameter setting method
99 and machine arrangement, the undercutting and secondary enveloping can be avoided in grinding
100 the screw rotor of a vacuum pump with concave profile. Deng and Shu [19] used space envelopment
101 theory to design the profile of forming tool, and introduced the design method of mounting
102 parameters. However, this method can only ensure that there is no interference between the forming
103 tool and the screw rotor. Unfortunately, no research has been conducted to correlate the setting
104 parameters with the cutting performance of the forming tool itself. Practical experience shows that
105 reasonable installation parameters can not only reduce the manufacturing cost of the forming tool,
106 but also improve the cutting performance of the forming tool, thereby improving the manufacturing
107 accuracy of the screw rotor and reducing the manufacturing cost.

108 Accordingly, this paper proposes a method to design mounting parameters of screw rotor forming
109 tools based on their machinability, in order to guarantee that the designed forming tool have
110 excellent cutting performance. First, the design method of forming tool and the associated forming
111 grinding method are introduced, which provides a theoretical basis for subsequent research.
112 Subsequently, a parametric optimization design program is designed to solve the forming tool
113 installation parameters that satisfy the spatial meshing principle, and the cutting performance of the
114 forming tool with various installation parameters was analyzed to obtain the reasonable mounting
115 parameters. Finally, the screw rotor forming grinding experiments were performed, and the
116 experimental results are in good agreement with the theoretical results, which demonstrates the
117 effectiveness of the screw rotor forming tool installation parameter design method proposed in this
118 paper.

119 **2. Theoretical background**

120 *2.1. The coordinate system relationship*

121 To obtain the installation parameter range that satisfies the spatial meshing relationship and forming
122 process requirements, is a prerequisite for the accurate design of screw rotor forming tool profile. To
123 achieve this, the numerical relationship between the coordinate systems of screw rotor and forming tool
124 needs to be established first. The discrete point of the shaft section of the screw rotor is (x_t, y_t) , and the
125 three-dimensional model representation can be described as:

$$126 \quad [X, Y, Z] = [x_t \cos\theta - y_t \sin\theta, x_t \sin\theta + y_t \cos\theta, p\theta] \quad (1)$$

127 where p is the screw parameter of the screw rotor determined by $p = S/2\pi$, and S in the formula represents
 128 the lead of the screw rotor.

129 Point (Z_c, R_t) is a point on the cross section of the forming tool shaft, as shown in Fig. 1, the three-
 130 dimensional structure of the forming tool can be described by the following equation [3]:

$$131 \quad [X_c, Y_c, Z_c] = [R_t \cos\phi, R_t \sin\phi, f(R_t)] \quad (2)$$

132 where X_c , Y_c , and Z_c are the 3d model equation of the forming tool; R_t is the radius when the width
 133 of the forming tool is Z_c ; ϕ is the angle between R_t and the plane $X_c O_c Z_c$; and the X_c to Y_c
 134 direction is defined as the positive direction.

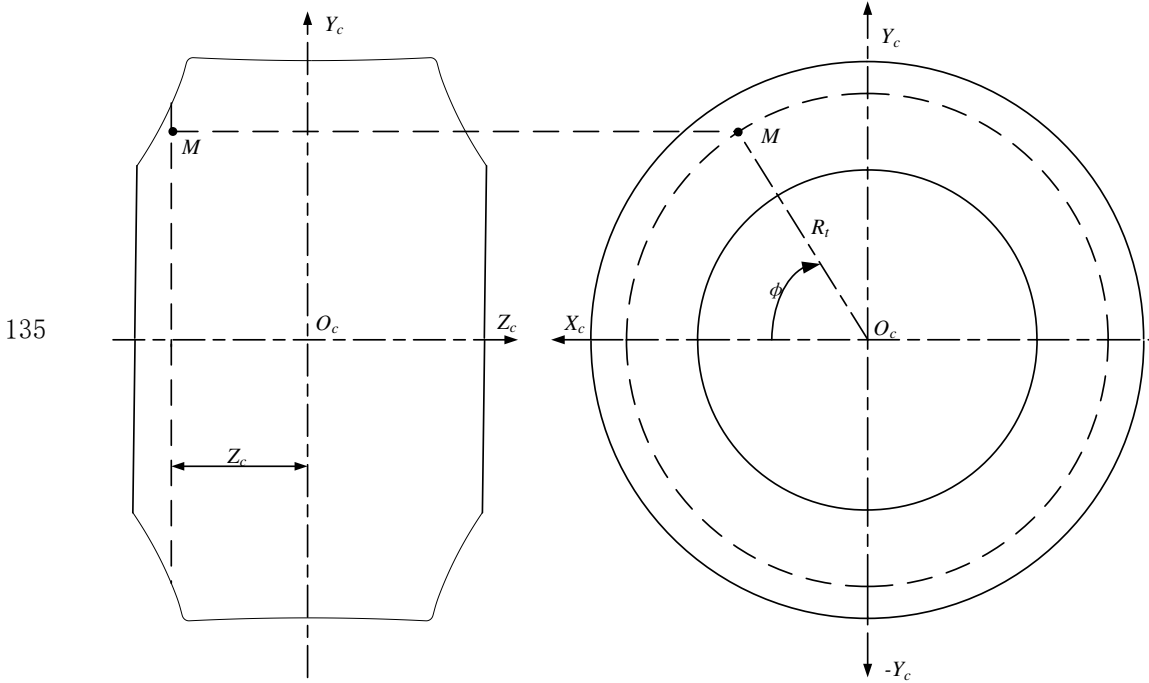


Fig. 1. Forming tool section diagram.

136
 137 During the forming process, the screw rotor profile is generated through space meshing motion
 138 between the forming tool and the screw rotor. The geometric relationship between a screw rotor and a
 139 forming tool as shown in Fig. 2 The rotating shafts of the screw rotor and the forming tool are spatially
 140 crossed, generating a setting angle ω . T is called the center distance, which is the distance between the
 141 forming tool axis and the screw rotor axis. The point M is a point on the space contact line between the
 142 screw rotor and the forming tool. $O - XYZ$ is the space coordinate system of screw rotor, while $O -$
 143 $X_c Y_c Z_c$ is the space coordinate system of forming tool.

144 The mutual transformation relationship between the space coordinate system $O - X_c Y_c Z_c$ of the
 145 forming tool and the space coordinate system $O - XYZ$ of the screw rotor is as follows:

$$146 \quad [X, Y, Y] = [X_c \cos\omega + Z_c \sin\omega, Y_c + T, Z_c \cos\omega - X_c \sin\omega] \quad (3)$$

$$147 \quad [\vec{i}, \vec{j}, \vec{k}] = [\cos\omega \vec{i}_c + \sin\omega \vec{k}_c, \vec{j}_c, \cos\omega \vec{k}_c - \sin\omega \vec{i}_c] \quad (4)$$

$$148 \quad [X_c, Y_c, Z_c] = [X \cos\omega - Z \sin\omega, Y - T, X \sin\omega + Z \cos\omega] \quad (5)$$

$$149 \quad [\vec{i}_c, \vec{j}_c, \vec{k}_c] = [\cos\omega \vec{i} - \sin\omega \vec{k}, \vec{j}, \cos\omega \vec{k} + \sin\omega \vec{i}] \quad (6)$$

150 where $\vec{i}_c, \vec{j}_c, \vec{k}_c$ are the unit vectors in the X_c, Y_c and Z_c directions; $\vec{i}, \vec{j},$ and \vec{k} are the unit vectors
 151 in the X, Y and Z directions.

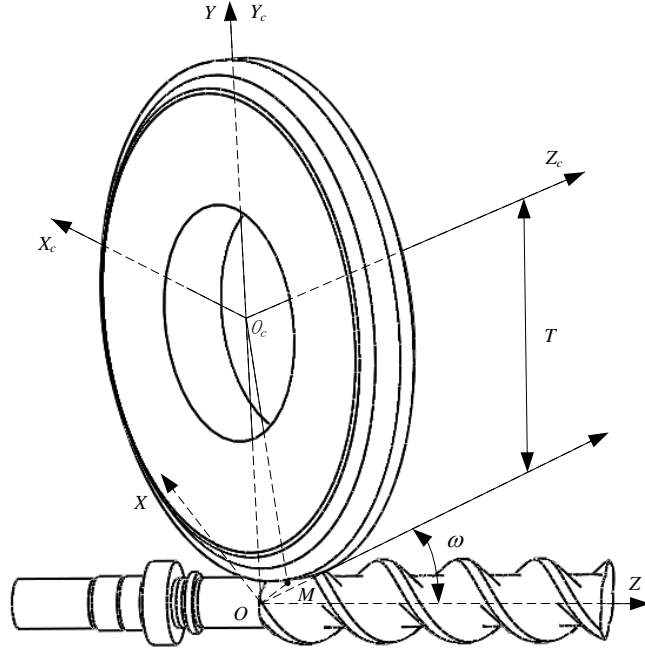


Fig. 2. Spatial position relationship between forming tool and screw rotor.

2.2. Forming tool profile computation model

When the three-dimensional model equation of the screw rotor is given, the profile equation of the forming tool can be obtained through a series of mathematical operations. The spatial contact line equation between the forming tool and the screw rotor can be expressed by the following equation [3]:

$$(\vec{k}_c \times \vec{R}) \cdot \vec{n} = 0 \quad (7)$$

where $\vec{R} = \overline{O_c M}$ is the radial vector of point M in spatial coordinate system $O - X_c Y_c Z_c$, and \vec{n} is the normal vector at point M in spatial coordinate system $O - XYZ$. The normal vector \vec{n} in spatial coordinate system $O - XYZ$ can be solved from the following equation:

$$\vec{n} = \frac{\partial \vec{r}}{\partial t} \times \frac{\partial \vec{r}}{\partial \theta} = \begin{vmatrix} \vec{i} & \vec{j} & \vec{k} \\ \frac{\partial X}{\partial t} & \frac{\partial Y}{\partial t} & \frac{\partial Z}{\partial t} \\ \frac{\partial X}{\partial \theta} & \frac{\partial Y}{\partial \theta} & \frac{\partial Z}{\partial \theta} \end{vmatrix} \quad (8)$$

By taking the partial derivatives of each component in Eq. (1), respectively, t and θ , the following equation can be established:

$$\begin{cases} \frac{\partial X}{\partial t} = \frac{dx_t}{dt} \cos \theta - \frac{dy_t}{dt} \sin \theta \\ \frac{\partial Y}{\partial t} = \frac{dx_t}{dt} \sin \theta + \frac{dy_t}{dt} \cos \theta \\ \frac{\partial Z}{\partial t} = 0 \end{cases} \quad (9)$$

$$\begin{cases} \frac{\partial X}{\partial \theta} = -x_t \sin \theta - y_t \cos \theta \\ \frac{\partial Y}{\partial \theta} = x_t \cos \theta - y_t \sin \theta \\ \frac{\partial Z}{\partial \theta} = p \end{cases} \quad (10)$$

By substituting Eqs. (9) and (10) into Eq. (8), the components of the normal vector \vec{n} can be solved:

$$169 \quad \begin{cases} n_x = p \left(\frac{dx_t}{dt} \sin\theta + \frac{dy_t}{dt} \cos\theta \right) \\ n_y = -p \left(\frac{dx_t}{dt} \cos\theta - \frac{dy_t}{dt} \sin\theta \right) \\ n_z = \left(\frac{dx_t}{dt} \cos\theta - \frac{dy_t}{dt} \sin\theta \right) (x_t \cos\theta - y_t \sin\theta) - (-x_t \sin\theta - y_t \cos\theta) \left(\frac{dx_t}{dt} \sin\theta + \frac{dy_t}{dt} \cos\theta \right) \end{cases} \quad (11)$$

170 Substituting Eqs. (5), (6) and (11) into Eq. (7) then yields:

$$171 \quad \begin{aligned} & [(x_t \cos\theta - y_t \sin\theta)(\cos\theta - K \sin\theta) + (x_t \sin\theta + y_t \cos\theta)(\sin\theta + K \cos\theta)] \\ & [Y - T - p \cot\omega] + [p(\cos\theta - K \sin\theta)] \cdot p\theta \\ & + [p(\sin\theta + K \cos\theta)] \cdot T \cot\omega = 0 \end{aligned} \quad (12)$$

172 where K is the first derivative of y_t versus x_t , which can be solved by MATLAB program. As can be
173 seen, angle θ is the only unknown variable, and it can be solved when T , ω , and the profile equation
174 of the screw rotor are given. Thus, the spatial contact line can be deduced, and the profile equation of the
175 forming tool can be solved.

176 2.3. Rotor profile computation model

177 Similarly, when the three-dimensional model equation of the forming tool is given, the profile equation
178 of the screw rotor can be obtained through a series of mathematical operations. The spatial contact line
179 equation between the screw rotor and the forming tool can be expressed by the following equation [3]:

$$180 \quad (\vec{k} \times \vec{r} + p\vec{k}) \cdot \vec{n} = 0 \quad (13)$$

181 where $\vec{r} = \overline{OM}$ is the radial vector of point M in spatial coordinate system $O - XYZ$. In the forming
182 tool spatial coordinate system $O - X_c Y_c Z_c$, the vector \vec{r} can be expressed in the following equation:

$$183 \quad \vec{r} = \vec{R} + T\vec{j}_c = R_t \cos\phi \vec{i}_c + R_t \sin\phi \vec{j}_c + f(R_t) \vec{k}_c + T\vec{j}_c \quad (14)$$

184 By introducing Eq. (6) into Eq. (14), in the spatial coordinate system $O - XYZ$ of screw rotor, the
185 vector \vec{r} can be represented as the following equation:

$$186 \quad \vec{r} = [R_t \cos\phi \cos\omega + f(R_t) \sin\omega] \vec{i} + (R_t \sin\phi + T) \vec{j} + [f(R_t) \cos\omega - R_t \cos\phi \sin\omega] \vec{k} \quad (15)$$

187 The term $\vec{k} \times \vec{r} + p\vec{k}$ can be deduced as follows:

$$188 \quad \vec{k} \times \vec{r} + p\vec{k} = [R_t \cos\phi \cos\omega + f(R_t) \sin\omega] \vec{j} - (R_t \sin\phi + T) \vec{i} + p\vec{k} \quad (16)$$

189 The normal vector \vec{n} can be deduced according the following equation:

$$190 \quad \vec{n} = \frac{\partial \vec{r}}{\partial R_t} \times \frac{\partial \vec{r}}{\partial \phi} = \begin{vmatrix} \vec{i} & \vec{j} & \vec{k} \\ \frac{\partial X}{\partial R_t} & \frac{\partial Y}{\partial R_t} & \frac{\partial Z}{\partial R_t} \\ \frac{\partial X}{\partial \phi} & \frac{\partial Y}{\partial \phi} & \frac{\partial Z}{\partial \phi} \end{vmatrix} \quad (17)$$

191 By taking the partial derivative of each item in Eq. (3), respectively, R_t and Z_c , the following
192 equations can be established:

$$193 \quad \begin{cases} \frac{\partial X}{\partial R_t} = \cos\phi \cos\omega + f'(R_t) \sin\omega \\ \frac{\partial Y}{\partial R_t} = \sin\phi \\ \frac{\partial Z}{\partial R_t} = f'(R_t) \cos\omega - \cos\phi \sin\omega \end{cases} \quad (18)$$

$$194 \quad \begin{cases} \frac{\partial X}{\partial \phi} = -R_t \sin\phi \cos\omega \\ \frac{\partial Y}{\partial \phi} = R_t \cos\phi \\ \frac{\partial Z}{\partial \phi} = R_t \sin\phi \sin\omega \end{cases} \quad (19)$$

195 By substituting Eqs. (18) and (19) into Eq. (17), the components of the normal vector \vec{n} can be solved:

$$196 \quad \begin{cases} n_x = R_t \sin\omega - f'(R_t) \cos\omega R_t \cos\phi \\ n_y = -f'(R_t) R_t \sin\phi \\ n_z = R_t \cos\omega + f'(R_t) \sin\omega R_t \cos\phi \end{cases} \quad (20)$$

197 Substituting Eqs. (16) and (20) into Eq. (13) then yields:

198
$$(T + p \tan \omega) \cos \phi - [f(R_t) + \frac{1}{f'(R_t)} R_t] \tan \omega \sin \phi + \frac{1}{f'(R_t)} (p - T \tan \omega) = 0 \quad (21)$$

199 where $f'(R_t)$ is the first derivative of Z_c versus R_t . Since each R_t corresponds to two different
200 values of Z_c , the R_t value can be considered as a function of Z_c , as shown in Fig. 1. The term
201 $1/f'(R_t)$ is deduced by the derivative rule for inverses:

202
$$\frac{1}{f'(R_t)} = [f^{-1}(Z_c)]' \quad (22)$$

203 Eq. (21) shows that angle ϕ is the only unknown variable; angle ϕ can be deduced according to T ,
204 ω , and the profile equation of the forming tool. Thus, the section profile of the screw rotor is further
205 obtained.

206 *2.4. Profile errors calculation method*

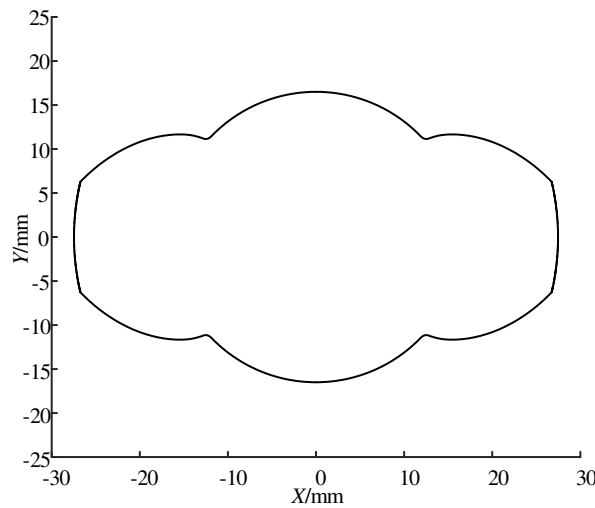
207 The definition of screw rotor profile error is the basis of studying the influence of mounting parameters
208 on screw rotor profile error. The axial section of screw rotor profile is shown in Fig. 3. By comparing the
209 difference between the processed profile and the theoretical profile, the profile error of the machined
210 profile can be obtained, as shown in Fig. 4. The coordinates of point C_i are denoted by (x_i, y_i) ($i =$
211 $\{1, 2, \dots, m\}$), where m is the number of points determined by the geometric size of the screw rotor and
212 the measuring accuracy of the measuring equipment. In this paper, the minimum distance between the
213 point C_i on the machined profile and the initial theoretical profile is defined as the profile error at the
214 point C_i , which is expressed by E_i . The profile error E_i is negative when point C_i is inside the
215 theoretical profile, and vice versa.

216 In order to facilitate the calculation of the profile error, the theoretical profile of the rotor can be fitted
217 by cubic parameter splines by MATLAB software as follows:

218
$$y = S(x) \quad (23)$$

219

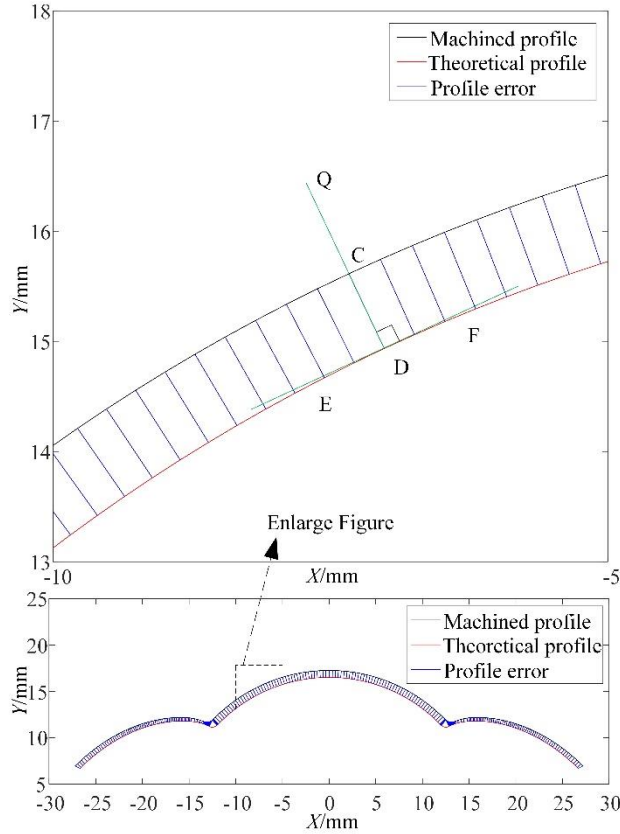
220



221

Fig. 3. Theoretical profile of screw rotor.

222



223

Fig. 4. Schematic diagram of profile error.

224

The profile error of point C_i on the machining profile can be obtained by the following formula:

225

$$E_i = \pm L_i(\min) \quad (24)$$

$$L_i(\min) = \sqrt{(x_i - x_k)^2 + (y_i - S(x_k))^2}$$

226

where points $(x_k, S(x_k))$ satisfy Eq. (23). If $(x_i^2 + y_i^2) > (x_k^2 + S(x_k)^2)$, when the machined profile is outside the theoretical profile, “+” is chosen; otherwise, “-” is chosen. The minimum distance, $L_i(\min)$, can be easily calculated using MATLAB software; Using this method, the profile error of any point on the machined profile can be accurately obtained.

230

3. Mounting parameter optimization decision method

231

In the screw rotor precision forming process, the mounting parameters of the forming tool not only determine its own design accuracy but also affect its own cutting performance. In Section 2, The mutual transformation relation between screw rotor and forming tool, and the calculation method of screw rotor profile error have been explained clearly. In view of the importance of mounting parameters to screw rotor forming tool, it is essential to pay attention to the selection strategy of mounting parameters. In this paper, a novel decision method of mounting parameters for screw rotor forming tool based was proposed on the principle of space meshing and the coordinate system mutual transformation between the forming tool and the screw rotor, and the screw rotor precision forming grinding was taken as an example.

239

3.1. Mounting angle range optimization decision method

240

In order to solve the mounting angle range that meets the process conditions, the mounting angle optimization design program is designed as shown in Fig. 5. During the actual grinding process of the screw rotor, the forming wheel radius becomes smaller and smaller with the increase of grinding time. In order to maximize the use of the abrasive on the forming wheel, the minimum installation center

241

242

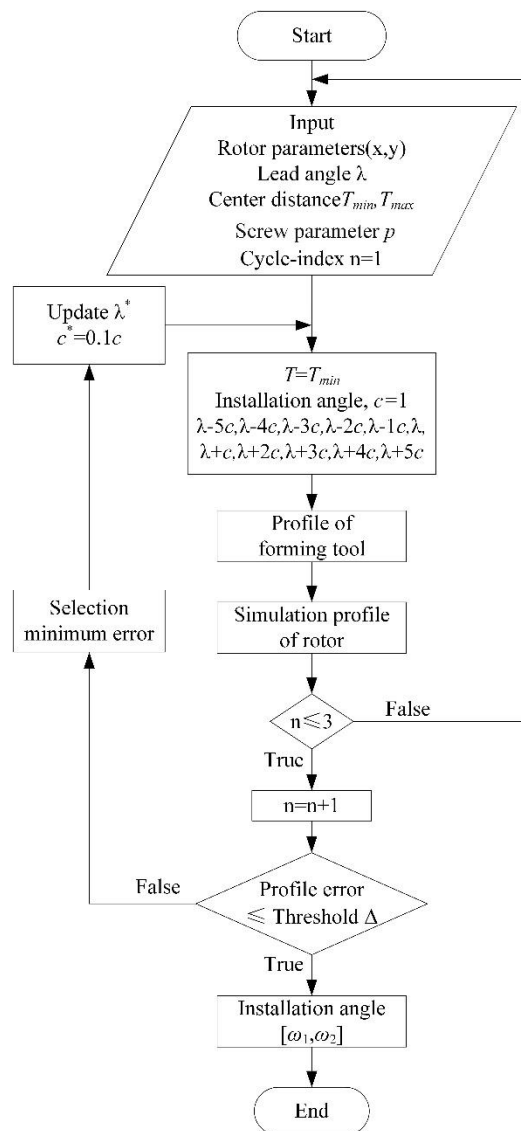
243

244 distance satisfying the process requirements is taken as the initial center distance parameter. Taking a
 245 certain type of male rotor as an example, its geometric parameters are shown in the following Table 1:
 246

Table 1. Geometrical parameters of a female rotor.

Item	Values
Tip diameter (mm)	54.94-54.95
Root diameter (mm)	33.00-33.01
Lead (mm)	108.00
Pitch diameter (mm)	33.00
Lead angle (°)	46.171
Profile tolerance (mm)	± 0.01
Screw direction	Right-handed

247



248

Fig. 5. Flowchart of installation angle optimization design.

249

The steps of the program for optimization of grinding wheel installation angle of screw rotor are as follows:

250

251

- Step 1. Input initial parameter, including discrete data points of screw rotor section profile, pitch circle lead angle, screw parameter, center distance, and cycle-index.

252

253

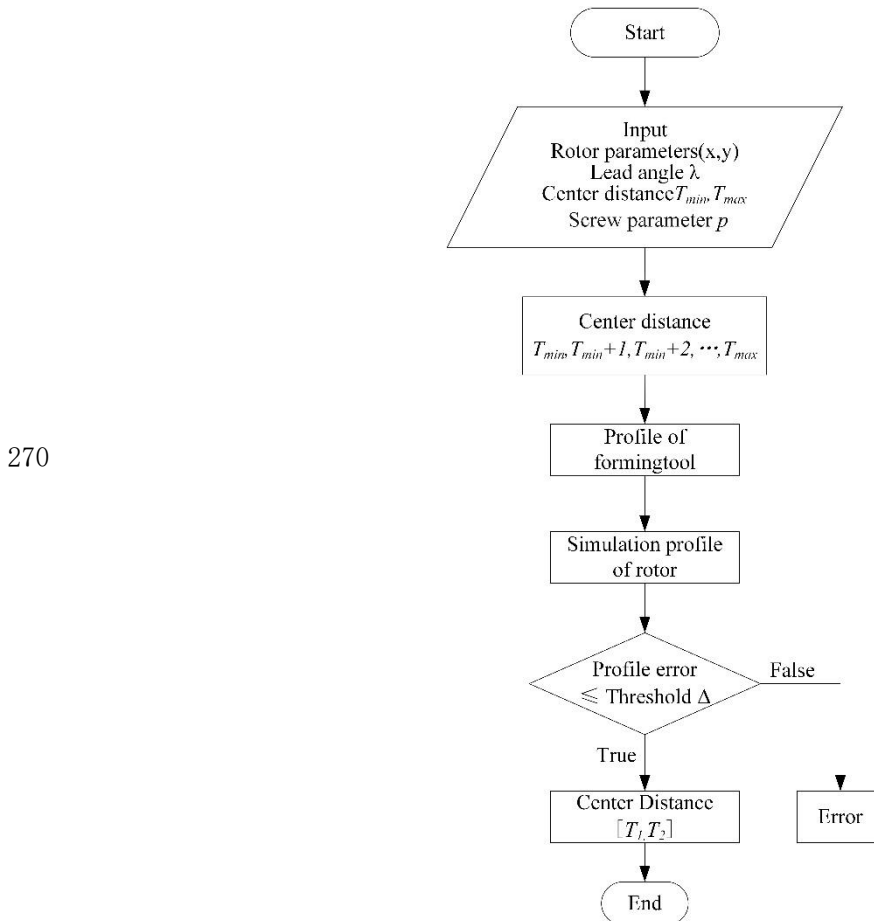
- Step 2. Set initial center distance and mounting angle.

- 254 • Step 3. Forming tool profile generation.
- 255 • Step 4. Screw rotor simulation profile generation.
- 256 • Step 5. If cycle-index n less than or equal to 3, the next step was executed; otherwise, it
- 257 returns to the first step.
- 258 • Step 6. The profile error of simulation profile of screw rotor was evaluated. When the
- 259 maximum value of the profile error \leq threshold Δ , the current mounting angle value would
- 260 be recorded; otherwise, return to step 2.

261 In the initial parameter setting, the range of the installation angle is limited to $[\lambda-5, \lambda+5]$, and the
 262 judgment condition is set as $E_{imax} \leq \Delta$. Through three cycles of optimization calculations, the precise
 263 mounting angle range that satisfies the conditions can be obtained.

264 3.2. Center distance range optimization decision method

265 Similarly, in order to solve the center distance range that meets the process conditions, the center
 266 distance optimization design program is designed as shown in Fig. 5. In the actual screw rotor grinding
 267 process, the installation center distance is usually determined by the structure of the grinding machine
 268 and the size of the forming grinding wheel. Therefore, center distance should be searched within the
 269 interval $[T_{min}, T_{max}]$. satisfying the structural parameters of machine tool and cutting tool.



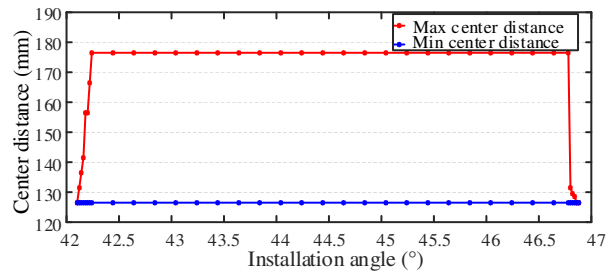
271 Fig. 6. Flowchart of center distance optimization design.

272 The steps of the program for optimization of grinding wheel installation center distance of screw rotor
 273 are as follows:

- 274 • Step 1. Input initial parameter, including discrete data points of screw rotor section profile,
- 275 pitch circle lead angle, center distance, and screw parameter.

- 276 • Step 2. Set initial center distance and mounting angle.
- 277 • Step 3. Forming tool profile generation
- 278 • Step 4. Screw rotor simulation profile generation
- 279 • Step 5. The profile error of simulation profile of screw rotor was evaluated. When the
- 280 maximum value of the profile error \leq threshold Δ , the current mounting angle was recorded;
- 281 otherwise, otherwise, prompt an error and end the program.

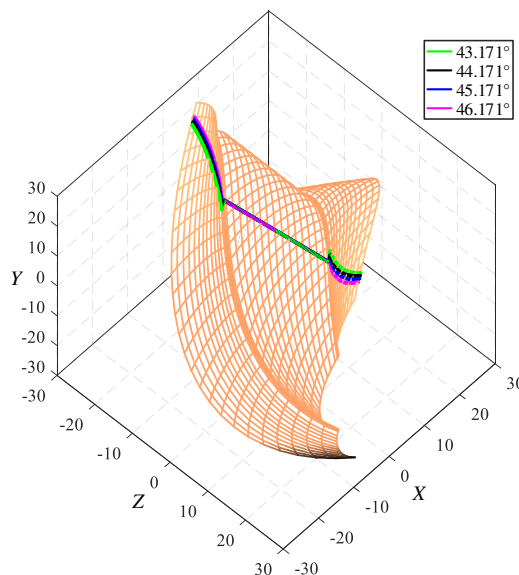
282 The mounting angle and center distance of the forming tool before the screw rotor forming process
 283 can be optimized by the method mentioned in this paper. The mounting parameters of the forming tool
 284 of the female screw rotor mentioned in Table 1 are shown in Fig. 7.



286 Fig. 7. Mounting parameters range of forming tool.

287 3.3. Profile characteristics analysis of forming tool

288 At any moment when the rotary surface of the forming tool moves relative to the screw surface of the
 289 screw rotor, there is always a tangent contact line between the two surfaces, as shown in Fig. 8, which is
 290 the most essential feature of forming grinding. In the process of screw rotor form grinding contact line
 291 can be considered to be the actual grinding blade. The forming tool keep axial fixed only around its own
 292 axis high-speed rotation. While the screw rotor performs linear and rotary composite motion, which is
 293 equivalent to the grinding wheel doing rotary cutting motion along the screw groove of the screw rotor,
 294 so as to cut off the excess material of the workpiece.

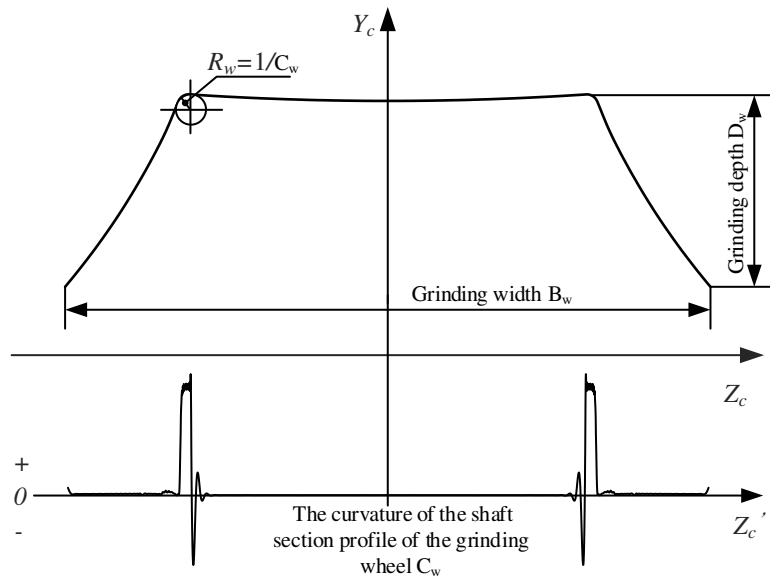


295
 296 Fig. 8. The shape and pose of space contact line

297 The forming tool profile is the projection of the contact line on the cross section of the grinding wheel
 298 shaft, so it can be seen that the shape and spatial pose of the contact line not only determine the spatial
 299 contact relationship between the grinding wheel and the screw rotor, but also determines the profile of

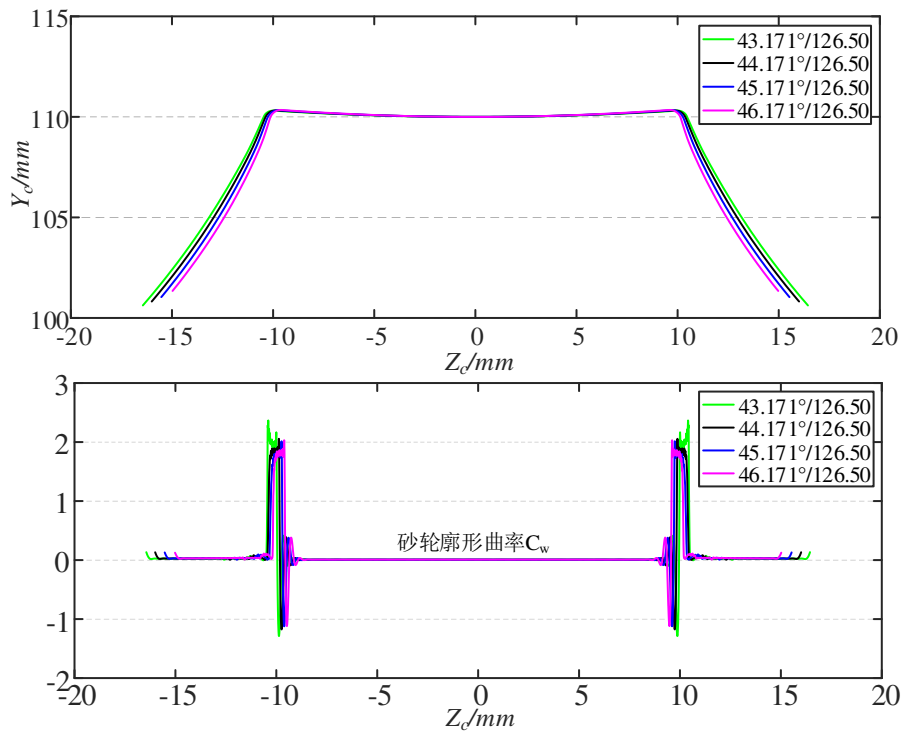
300 the grinding wheel. Therefore, the precision grinding quality of screw rotor is closely related to the shape
 301 and position of the spatial contact line.

302 In order to obtain the mounting parameters that match the processing requirements, it is necessary to
 303 carry out further in-depth research on the profile characteristics of the forming tool under different
 304 mounting parameters. In order to evaluate the cutting performance of the forming tool under different
 305 mounting parameters, the cutting performance evaluation system of the forming tool should be
 306 established first, as shown in Fig. 9.



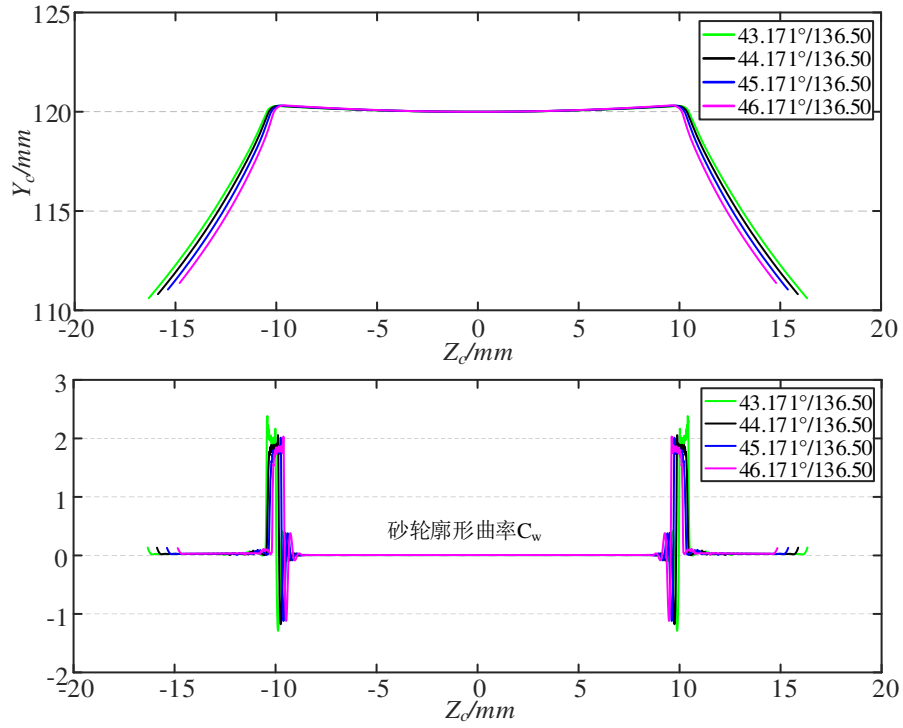
307
 308

Fig. 9 The evaluation system of forming tool profile

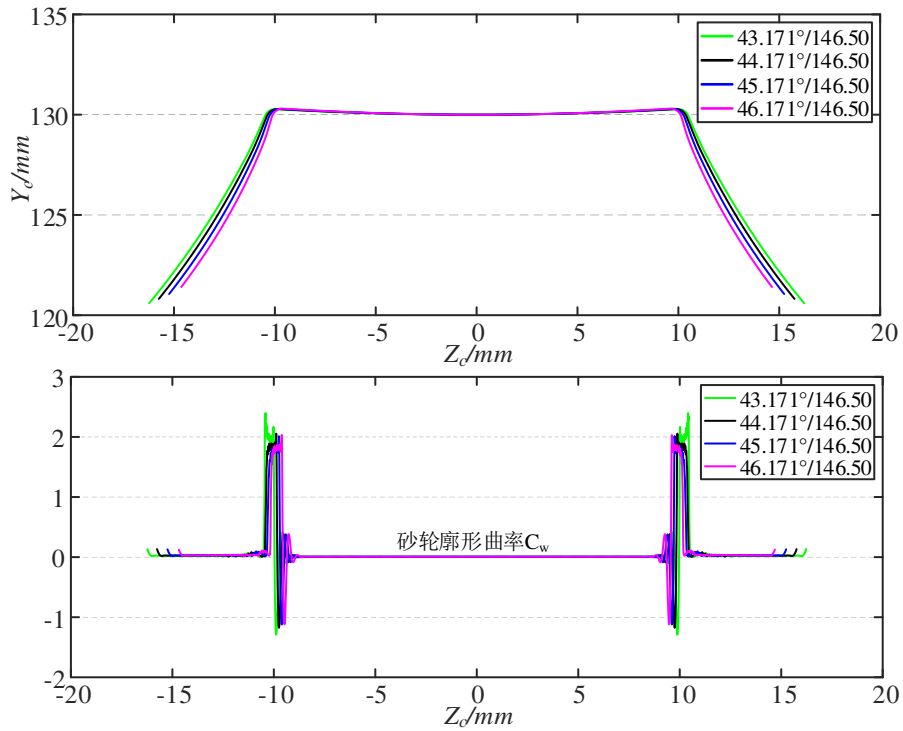


309
 310

a) Center distance 126.50mm



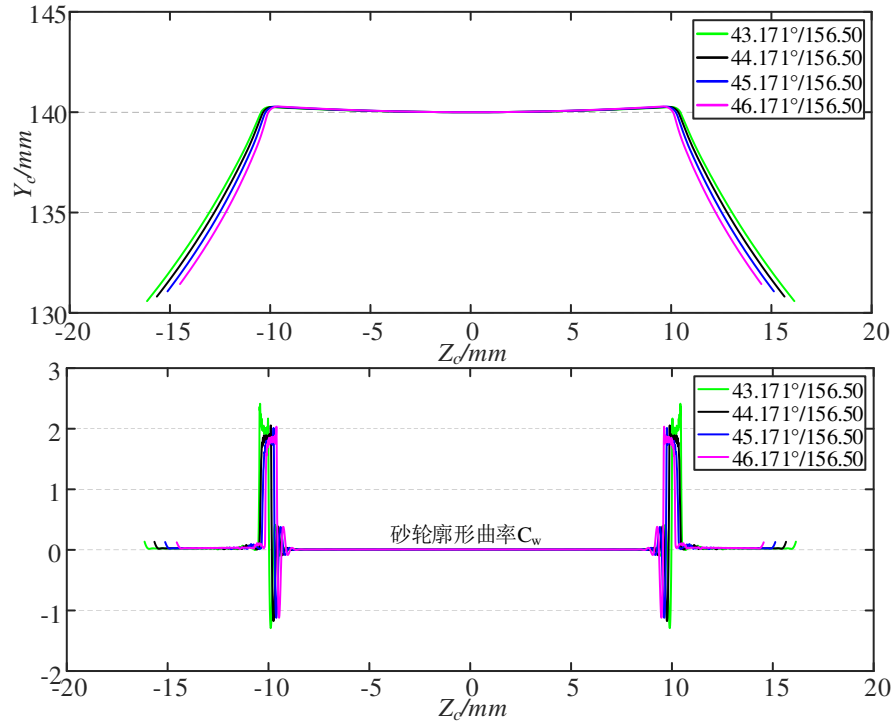
b) Center distance 136.50mm



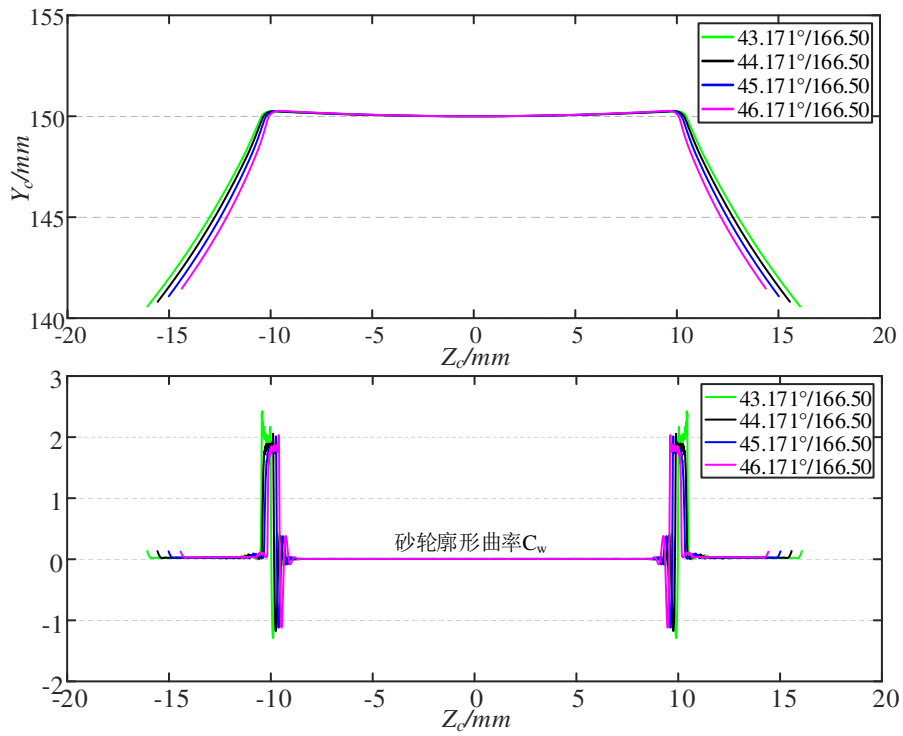
c) Center distance 146.50mm

311
312
313

314
315
316



d) Center distance 156.50mm



e) Center distance 166.50mm

317

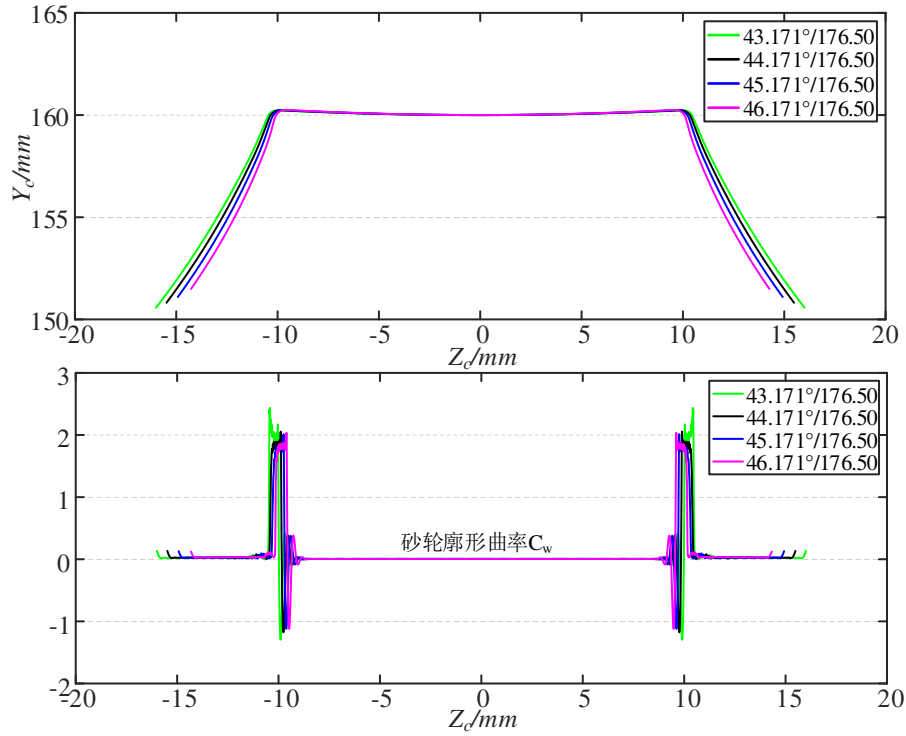
318

319

320

321

322



f) Center distance 176.50mm

Fig.10. Profile characteristics of forming tool

323
324
325
326

327 The following information can be derived from Fig. 10. When the center distance between the screw
328 rotor and the forming tool remains constant, the maximum profile curvature of the forming tool decreases
329 slightly with the increase of the mounting angle of the grinding wheel, and the maximum curvature
330 appears at the transition place between the outer circle and the side of the grinding wheel. However, when
331 the mounting angle between the forming tool and the screw rotor remains stable, the profile curvature of
332 the forming tool remains stable even if the center distance between the screw rotor and the formed
333 grinding wheel changes. According to practical experience, the larger the curvature of forming grinding
334 profile, the faster the grinding wheel will wear. In addition, from the perspective of manufacturing, the
335 smaller the curvature of shaped sand profile, the lower the manufacturing cost.

336
337

The wear rate k , expressed below as Eq. (23) and defined as the ratio of the grinding wheel wear
volume to the material volume removed from the workpiece.

338

$$k = \frac{V_w}{V_s} = \frac{2\pi R_w S_w}{L_s S_s} \quad (23)$$

339
340
341

where R_w , L_s are respectively the radius of grinding wheel and the length of rotor helix at the contact
point between forming tool and workpiece. S_w , S_s are the wear unit area of grinding wheel and
workpiece at their contact point.

342
343
344
345
346

When the grinding parameters (grinding speed, cutting depth, cooling conditions, etc.) remain
unchanged, k and L_s remain unchanged. Therefore, when the grinding wheel radius R_s is smaller, the
grinding wheel wear unit area is larger. As a result, the smaller the grinding wheel radius is, the faster the
grinding wheel wear will be, and the grinding wheel needs to be dressed more frequently, leading to the
reduction of grinding efficiency.

347
348

On the other hand, the grinding width of the grinding wheel decreases as the mounting angle increases
when the center distance remains unchanged. As can be seen from Fig. 10, when the mounting angle is

349 46.171°, the maximum grinding width of the grinding wheel is 16.1mm. However, when the mounting
 350 angle is 46.171°, the maximum grinding width of the grinding wheel is 13.9mm, and the corresponding
 351 cost of the grinding wheel is saved by more than 13%.

352 In summary, through the analysis of screw rotor profile characteristics under different mounting
 353 parameters, the following conclusions can be known. Different mounting parameters between the screw
 354 rotor and the grinding wheel correspond to different profile characteristics of the forming wheel and have
 355 different grinding performance. Compared with the center, the mounting angle has a more obvious effect
 356 on the profile characteristics of the forming tool. In order to make full use of the grinding wheel, the
 357 mounting angle should be determined in priority. Different mounting angle will lead to different width
 358 of grinding wheel, so that the screw rotor manufacturing cost is different. When the above factors are
 359 taken into account, a smaller mounting angle should be selected to achieve precision form processing of
 360 the screw rotor with a lower cost.

361 4. Experiment and Results

362 4.1. Experimental setup

363 In order to verify the effectiveness and feasibility of the proposed mounting parameter decision method
 364 of screw rotor forming grinding wheel, a set of experiments on screw rotor forming grinding were
 365 designed. The equipment used in the experiment was shown in Table 4. as shown in Fig. 11. The screw
 366 rotor used was Y40Mn (HB 190-210). The screw rotor material in the experiment is Y40Mn in
 367 accordance with the actual application, and the hardness is HB170. The mounting parameters of the
 368 forming grinding wheel in the experiment are shown in Table 5.

369 Table 4. Experimental equipment

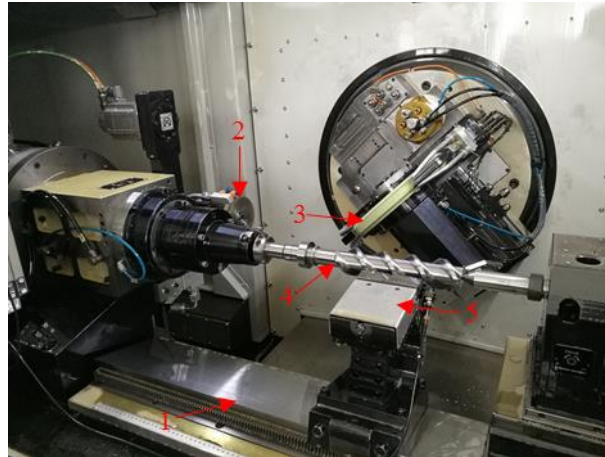
No	Setup	Brand	Model
1	Machine tool	Star SU	G 500 H Profile Grinding Machine
2	Grinding wheel	NORTON	3NQ60-H12VSP
3	Cutting fluid	Variocut	G600HC
4	Measuring equipment	Klingelnberg	P26

370

371 Table 5. Mounting parameters

No	center distance (mm)	mounting angle (°)
1	176.500	43.171
2	176.500	44.171
3	176.500	45.171
4	176.500	46.171
5	136.500	46.171
6	156.500	46.171

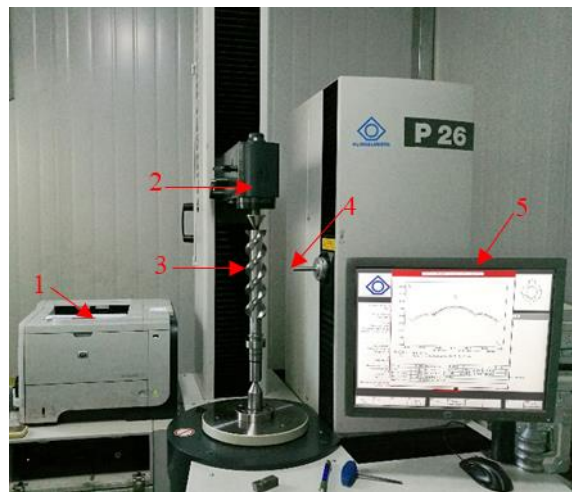
372



(1) Worktable. (2) Diamond dressing wheel.

(3) Grinding wheel. (4) Screw rotor. (5) Auxiliary supporting

Figure. 10 Grinding experimental setup



1. Printing mechanism 2. Clamping device 3. Screw rotor
4. Measuring head 5. Display instrument

Fig. 11 The fully automatic CNC-controlled P 26 precision measuring center

4.2 Results and discussion

To minimize the effects of grinding wheel wear on the accuracy of experimental results, the grinding wheel was modified before each grinding experiment. The profile error of the screw rotor is measured in the middle position. The results of the six experiments are shown in Appendix, where the actual profile measured from experiment and set theoretical profile are also compared. Compared with the theoretical profile, the error of most positions of each helical groove are within the tolerance band ± 0.01 mm. This means that the design method of mounting angle and center distance in this paper is accurate and reliable. In addition, the experimental results show that the error distribution trend of screw rotor is consistent with the slope and curvature distribution trend of forming grinding wheel. The largest error of profile appears at the transition between arc segment (root) and cycloid segment (side), which is also the position with the largest curvature and slope on the forming grinding wheel. It is also observed that as the radius of grinding wheel becomes smaller, the actual machining profile of screw rotor tends to be larger. The reason behind this is fewer abrasive particles will distribute on the surface as the of the radius of grinding wheel gets smaller, thus leading to faster wear of abrasive particles.

395 **5. Conclusion**

396 A novel design method for the mounting parameters of screw rotor forming grinding wheel
397 considering the cutting performance of forming grinding wheel was proposed in this paper. The
398 optimum design program of mounting angle and center distance has been developed. Based on the
399 established optimum design program, the range of mounting angle and center distance satisfying
400 the spatial meshing relationship is solved. Furthermore, the profile characteristics (cutting
401 performance) of the grinding wheel under different mounting parameters were investigated. The
402 numerical cases showed that the mounting angle had a significant effect on the profile characteristics
403 (cutting performance) of the forming grinding wheel. However, the center distance had little effect
404 on the profile characteristics (cutting performance) of the forming wheel. Nonetheless, when the
405 center distance becomes smaller, the grinding wheel radius becomes smaller, and the grinding wheel
406 wear becomes faster. Grinding experiments for male rotor with different mounting parameters were
407 performed to validate the results of the numerical cases. Some important conclusions are drawn as
408 follows:

- 409 (1) A novel model for calculating the mounting parameters of screw rotor forming grinding wheel
410 has been established based on the spatial engagement principle. The range of mounting
411 parameters satisfying the meshing principle and grinding equipment process parameters were
412 obtained
- 413 (2) The profile characteristics (cutting performance) of forming grinding wheel under different
414 mounting parameters were investigated. The relationship between the slope, curvature and
415 width of the shaft section profile of the grinding wheel and the mounting parameters of forming
416 grinding wheel were clarified. The mounting angle which has the greatest influence on the
417 profile characteristics of the forming grinding wheel should be controlled in priority.
- 418 (3) When pursuing grinding efficiency, a smaller mounting angle should be chosen because a larger
419 grinding wheel width can improve the stability of the grinding system. When pursuing grinding
420 quality and economy, a larger mounting angle should be selected, because a larger mounting
421 angle can reduce the slope and curvature of the grinding wheel profile, while reduce the width
422 of the grinding wheel to save the cost of the grinding wheel.

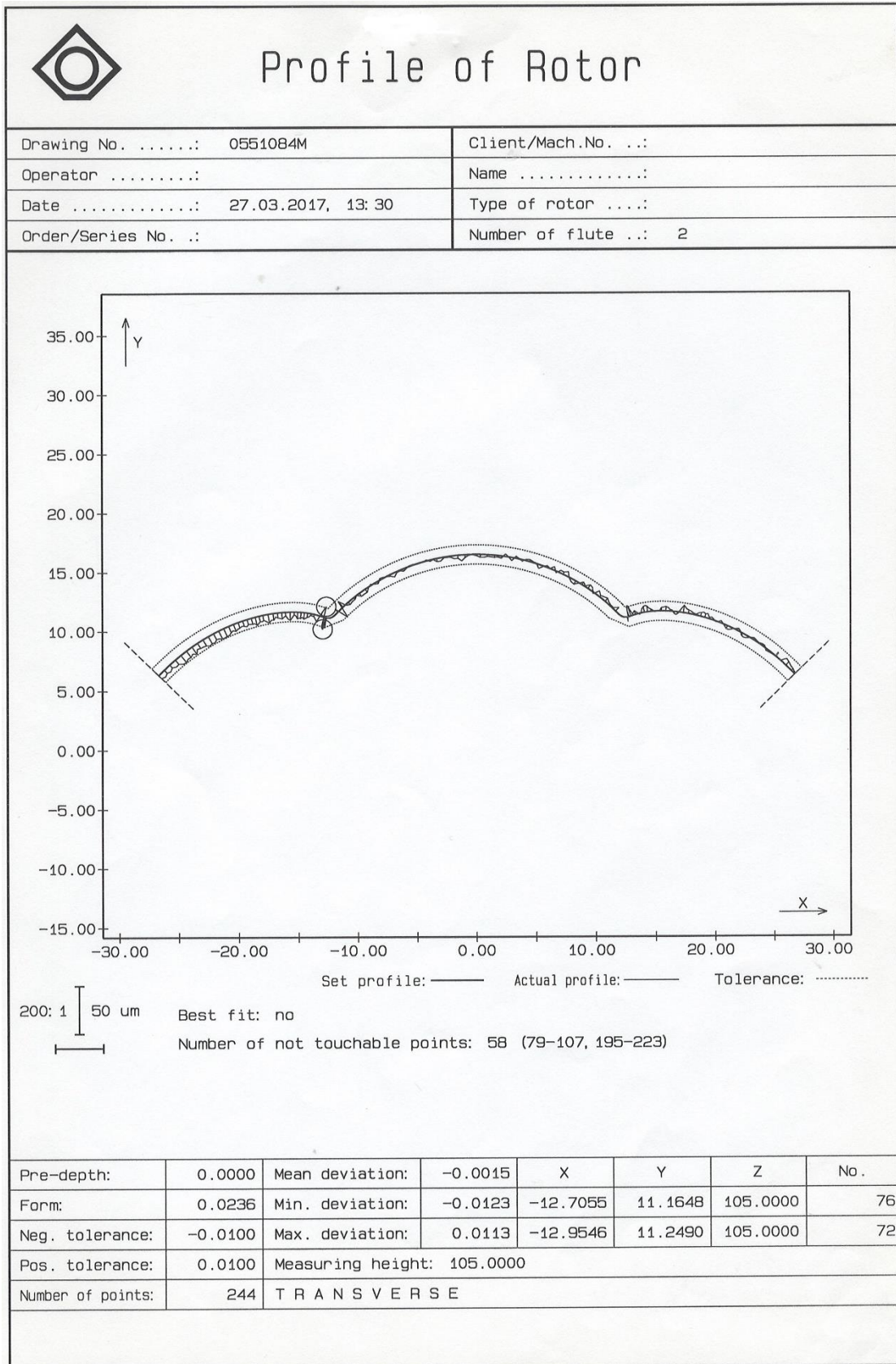
423 The above conclusions show that the mounting parameter design method accurate and reliable for
424 screw rotor forming grinding. In this paper, a method based on the cutting performance of the tool
425 is proposed for the design of tool mounting parameters in screw rotor forming machining, which
426 provides a theoretical basis for the selection of unmounted parameters and avoids the unreliability
427 of empirical method. In future work, this optimization design method can be extended and applied
428 to other types of forming processes. This method can also be integrated into the forming machine
429 system to improve the machining quality and efficiency of the machine.

430
431

432 **Declarations**

433 **Funding** This work was financially supported by The National Key Research and Development
434 Program of China (grant number 2018YFB1701203), the Doctoral Funding of Chongqing
435 University of Chongqing Technology and Business University (grant number 1956029), The
436 opening project of the international joint research center for health care in service of China-Canada
437 equipment system (grant number KFJJ2019061), Scientific research project of Chongqing

438 Technology and Business University (No. 2152015), Key research platform research team project
439 of Chongqing Technology and Business University (No.ZDPTTD201918)
440 **Competing interests** The authors declare no competing interests.
441 **Availability of data and material** The authors confirm that the data supporting the findings of this
442 study are available within the article.
443 **Code availability** Not applicable.
444 **Ethics approval** Not applicable.
445 **Consent to participate** Not applicable.
446 **Consent for publication** The manuscript is approved by all the authors for publication.
447 **Authors' contributions** All authors contributed to the study conception and design. Zongmin Liu
448 performed the data analyses and wrote the manuscript. Jirui Wang performed the experiment. Ning
449 Liu contributed significantly to analysis and manuscript preparation. Qian Tang and Bin Xing helped
450 perform the analysis with constructive discussions. All authors read and approved the final
451 manuscript.



453

454

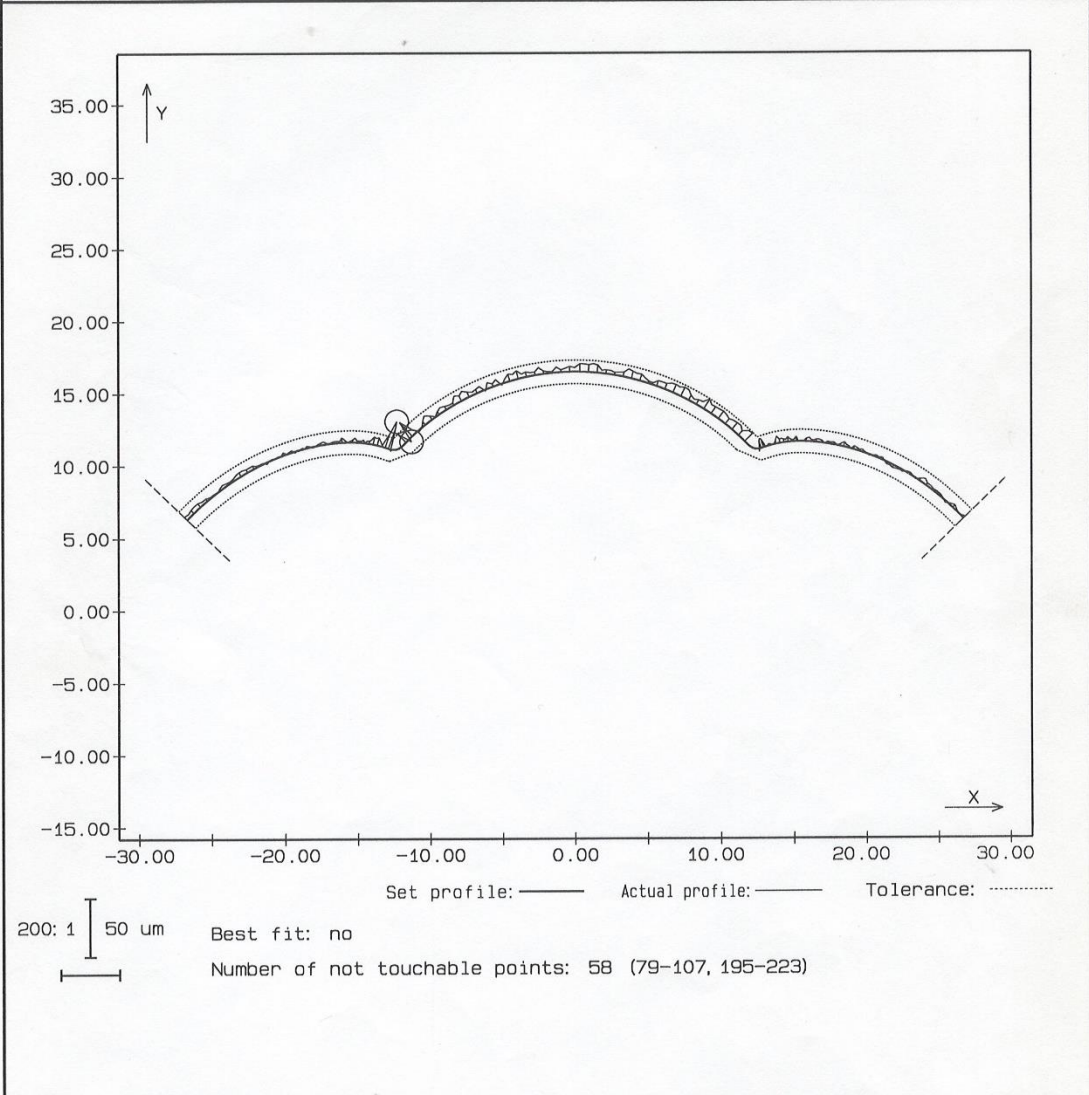
455

a) Center distance 176.500, mounting angle 43.171



Profile of Rotor

Drawing No.:	0551084M	Client/Mach.No. ...:	
Operator		Name	
Date	27.03.2017, 11:07	Type of rotor:	
Order/Series No. ..:		Number of flute ..:	1,2



Pre-depth:	0.0000	Mean deviation:	0.0029	X	Y	Z	No.
Form:	0.0271	Min. deviation:	-0.0031	-11.4516	11.8776	105.0000	109
Neg. tolerance:	-0.0100	Max. deviation:	0.0240	-12.9546	11.2490	105.0000	72
Pos. tolerance:	0.0100	Measuring height:	105.0000				
Number of points:	244	T R A N S V E R S E					

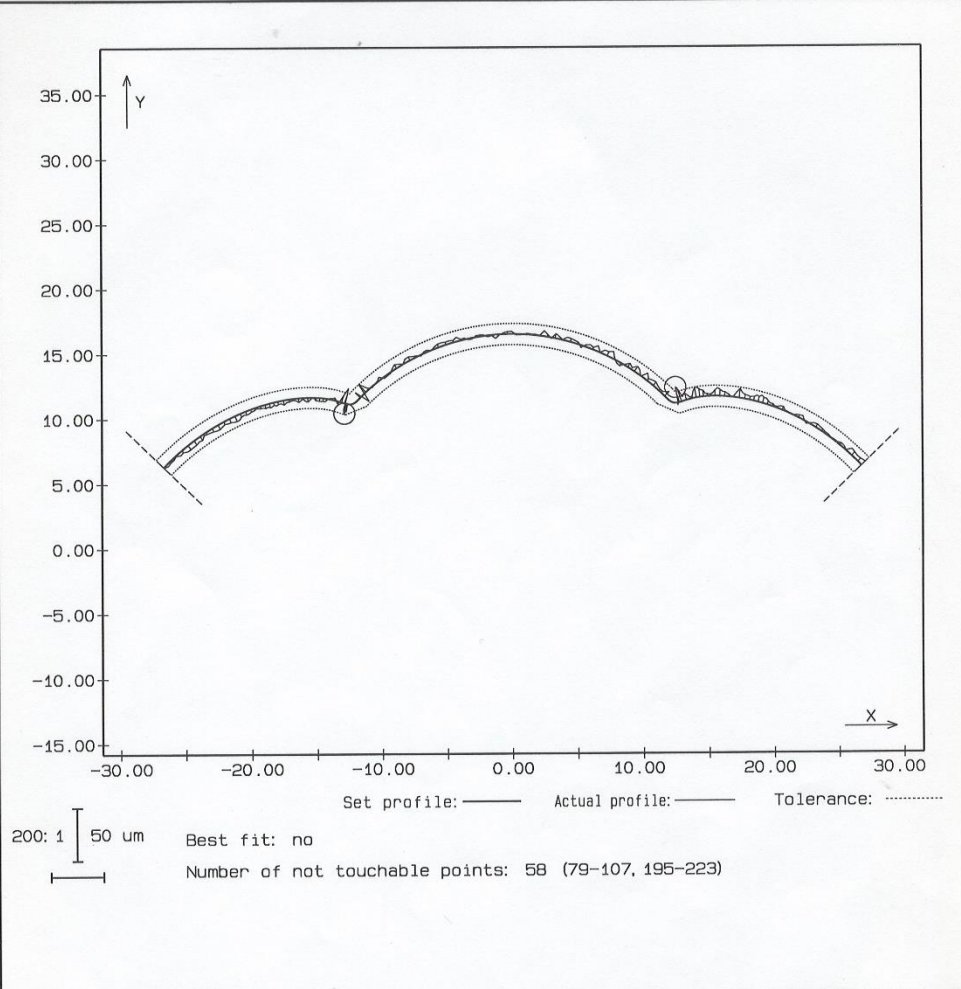
456
457

b) Center distance 176.500, mounting angle 44.171



Profile of Rotor

Drawing No.:	0551084M	Client/Mach.No. ...:	
Operator		Name	
Date	27.03.2017, 13:30	Type of rotor:	
Order/Series No. ..:		Number of flute ...:	1, 2



Pre-depth:	0.0000	Mean deviation:	0.0010	X	Y	Z	No.
Form:	0.0240	Min. deviation:	-0.0092	-12.7055	11.1648	105.0000	76
Neg. tolerance:	-0.0100	Max. deviation:	0.0148	12.8886	11.2259	105.0000	229
Pos. tolerance:	0.0100	Measuring height: 105.0000					
Number of points:	244	T R A N S V E R S E					

458

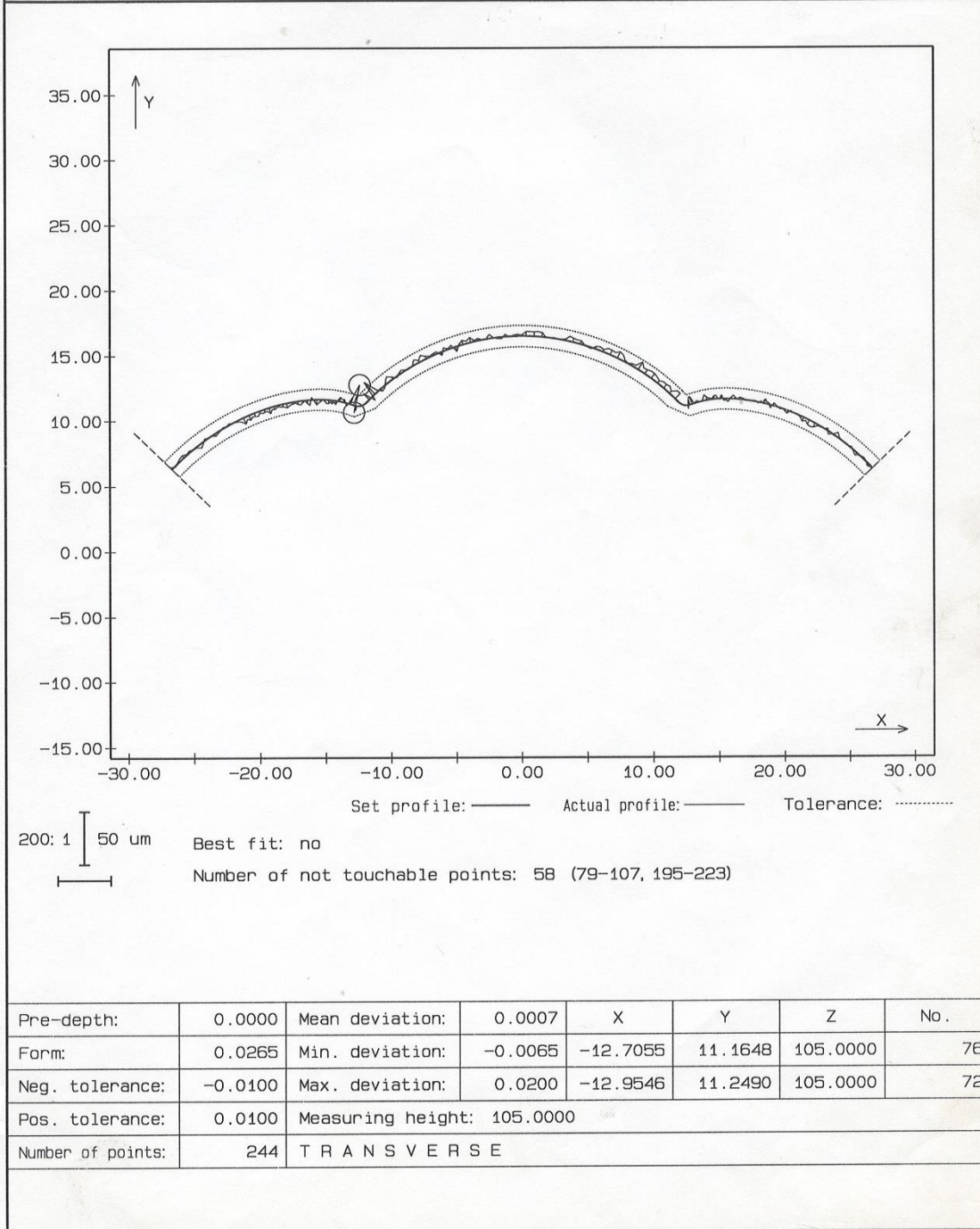
459

c) Center distance 176.500, mounting angle 45.171



Profile of Rotor

Drawing No.: 0551084M	Client/Mach.No. ...:
Operator	Name
Date: 27.03.2017, 11:07	Type of rotor:
Order/Series No. .:	Number of flute ..: 1



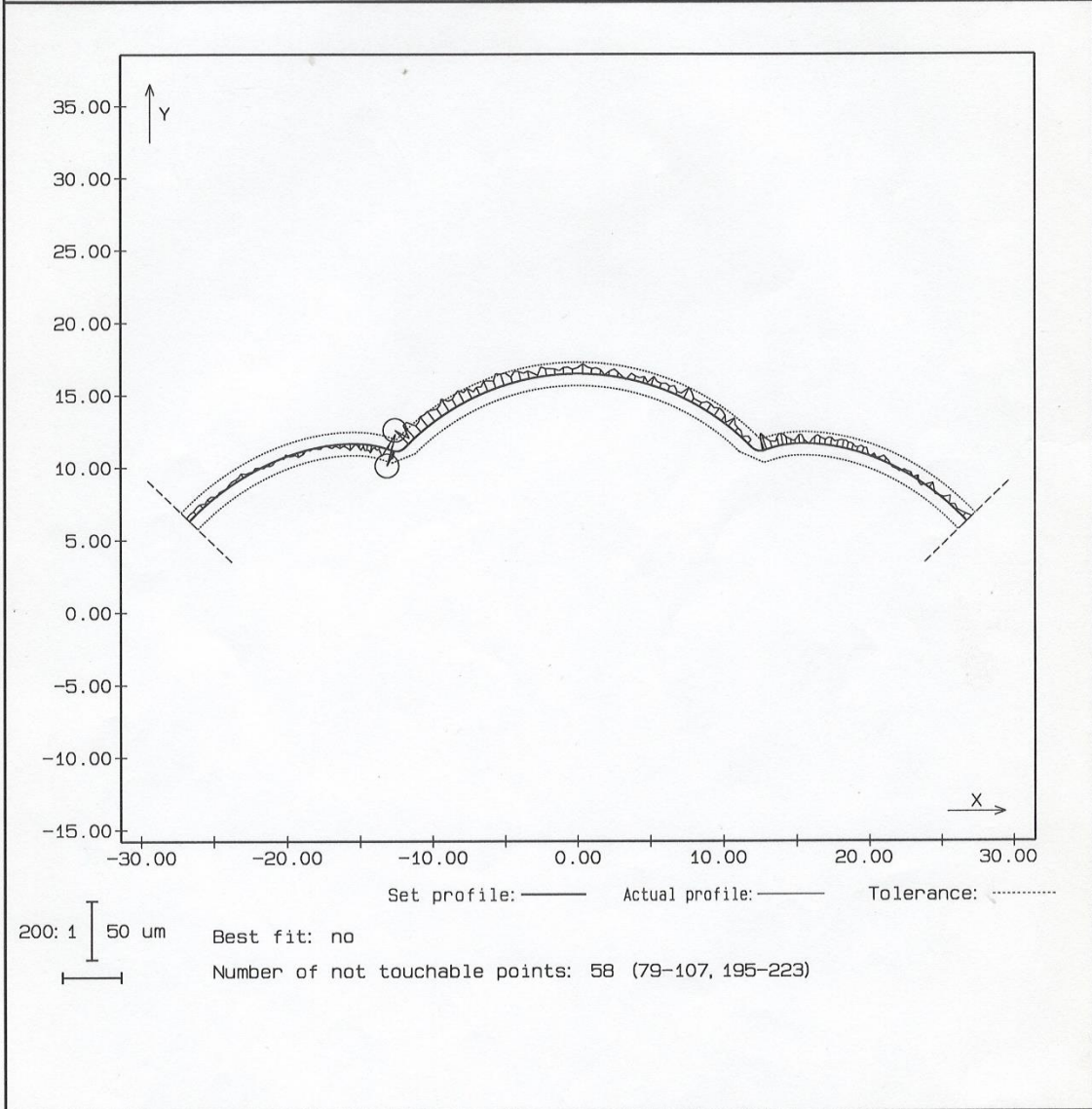
460
461
462

d) Center distance 176.500, mounting angle 46.171



Profile of Rotor

Drawing No.: 0551084M	Client/Mach.No. ...:
Operator	Name
Date: 27.03.2017, 12:51	Type of rotor:
Order/Series No. .:	Number of flute ..: 1



Pre-depth:	0.0000	Mean deviation:	0.0033	X	Y	Z	No.
Form:	0.0301	Min. deviation:	-0.0137	-12.7933	11.1922	105.0000	74
Neg. tolerance:	-0.0100	Max. deviation:	0.0165	-11.6657	11.6673	105.0000	108
Pos. tolerance:	0.0100	Measuring height: 105.0000					
Number of points:	244	T R A N S V E R S E					

463

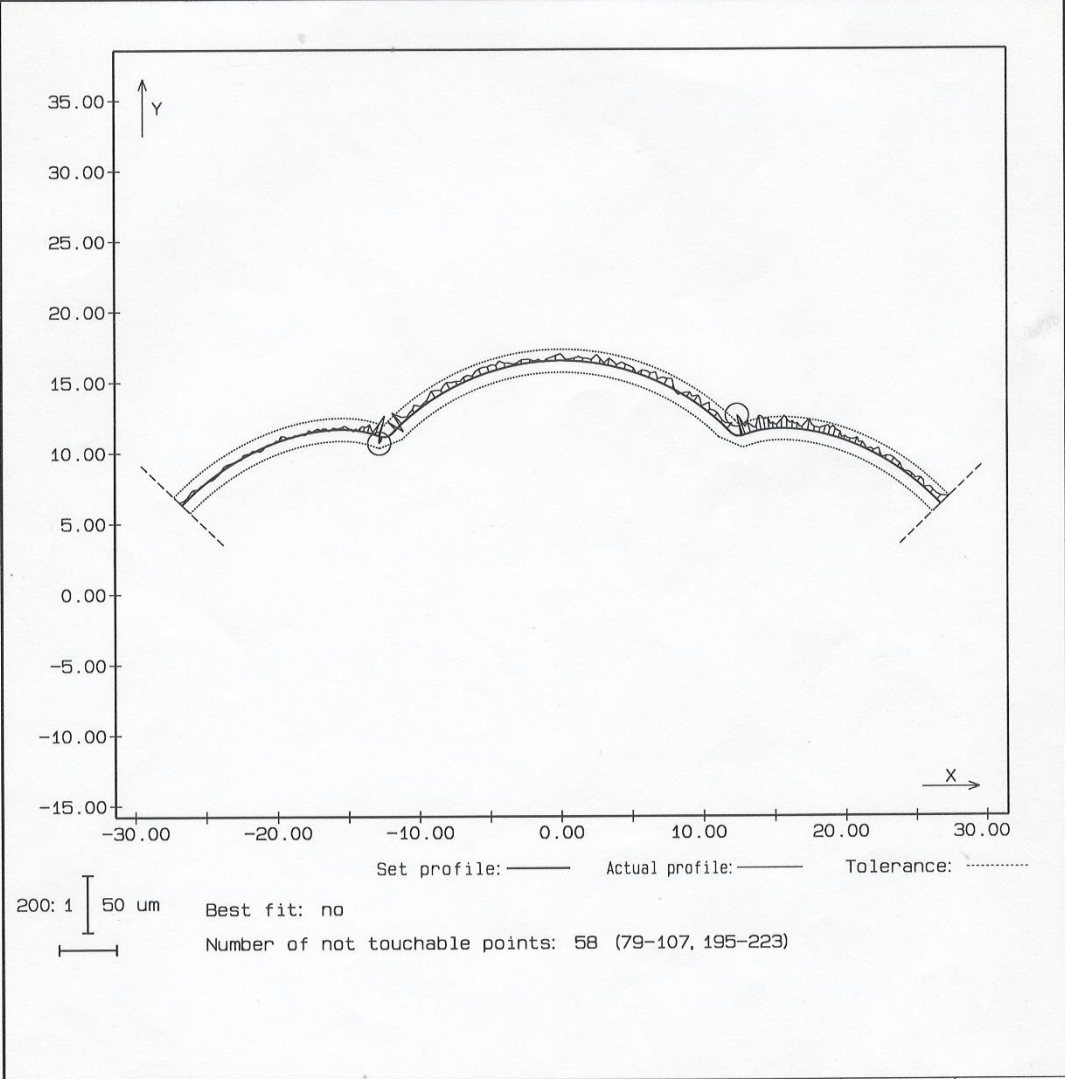
464

d) Center distance 136.500, mounting angle 46.171



Profile of Rotor

Drawing No.: 0551084M	Client/Mach.No. ..:
Operator	Name
Date	Type of rotor:
Order/Series No. .:	Number of flute ..: 1



Pre-depth:	0.0000	Mean deviation:	0.0035	X	Y	Z	No.
Form:	0.0244	Min. deviation:	-0.0060	-12.7055	11.1648	105.0000	76
Neg. tolerance:	-0.0100	Max. deviation:	0.0183	12.8886	11.2259	105.0000	229
Pos. tolerance:	0.0100	Measuring height:	105.0000				
Number of points:	244	T R A N S V E R S E					

465
466
467
468

f) Center distance 156.500, mounting angle 46.171

Fig. 12 The results of the six experiments

469 **References**

- 470 [1] Kovacevic A, Stosic N, Mujic E, Smith IK (2007) CFD integrated design of screw compressors,
471 Eng. Appl. Comput. Fluid Mech. 1:96–108.
- 472 [2] Litvin FL, Fuentes A (2004) Gear geometry and applied theory , Cambridge University Press.
- 473 [3] Wu X (2009) Theory of gearing, Xi'an Jiaotong University Press, (in Chinese).
- 474 [4] Tang Q, Zhang Y, Jiang Z, Yan D (2015) Design method for screw form cutter based on tooth
475 profile composed of discrete points. J Mech Des 137:085002.
- 476 [5] Wu YR, Fong ZH, Zhang ZX (2010) Simulation of a cylindrical form grinding process by the radial-
477 ray shooting (RRS) method. Mech Mach Theory 45:261–272.
- 478 [6] Li G (2017) A new algorithm to solve the grinding wheel profile for end mill groove machining. Int
479 J Adv Manuf Technol 90:775–784.
- 480 [7] Hoang MT, Wu YR, Tran VQ (2020) A general mathematical model for screw-rotor honing using
481 an internal-meshing honing machine. Mech Mach Theory 154:104038.
- 482 [8] Bizzarri M, Bartoň M (2021) Manufacturing of screw rotors via 5-axis double-flank cnc machining.
483 Comput Aided Des 132:102960.
- 484 [9] Stosic N (2006) Evaluating errors in screw rotor machining by tool to rotor transformation. Proc
485 Inst Mech Eng Part B J Eng Manuf 220:1589–1596.
- 486 [10] Stosic N (2006) A geometric approach to calculating tool wear in screw rotor machining. Int J Mach
487 Tools Manuf 46:1961–1965.
- 488 [11] Tao L, Wang Y, He Y, Feng H, Ou Y, Wang X (2016) A numerical method for evaluating effects of
489 installation errors of grinding wheel on rotor profile in screw rotor grinding. Proc Inst Mech Eng.
490 Part B J Eng Manuf 230:1381–1398.
- 491 [12] Zhao, Y, Zhao, S, Wei, W, Hou, H. Precision grinding of screw rotors using CNC method. Int J. Adv
492 Manuf Technol 89:2967–2979.
- 493 [13] Hoang MT, Wu YR (2021) Error compensation method for milling single-threaded screw rotors
494 with end mill tools. Mech Mach Theory 157:104170.
- 495 [14] Xiang S, Li H, Deng M, Yang J (2018) Geometric error analysis and compensation for multi-axis
496 spiral bevel gears milling machine. Mech Mach Theory 121:59–74.
- 497 [15] Ding H, Tang J, Zhong J (2016) Accurate nonlinear modeling and computing of grinding machine
498 settings modification considering spatial geometric errors for hypoid gears. Mech Mach Theory
499 99:155–175.
- 500 [16] Shih YP, Chen SD (2012) A flank correction methodology for a five-axis CNC gear profile grinding
501 machine, Mech Mach Theory 47:31–45.
- 502 [17] Liu Z, Tang Q, Liu N, Song J. (2019) A profile error compensation method in precision grinding of
503 screw rotors. Int J. Adv Manuf Technol 100:2557–2567.
- 504 [18] Zhang ZX, Fong ZH (2015) A novel tilt form grinding method for the rotor of dry vacuum pump.
505 Mech Mach Theory 90:47–58.
- 506 [19] Deng D, Shu P (1982) Rotary Compressor. China Machine Press, (in Chinese).